Journal of Organometallic Chemistry, 478 (1994) 161–171

A pictorial MO description of Buckminsterfullerene and its interactions with transition metal fragments

José A. López and Carlo Mealli

Istituto per lo Studio della Stereochimica ed Energetica dei Composti di Coordinazione (ISSECC, CNR), Via J. Nardi 39, 50132 Firenze (Italy)

(Received November 8, 1993)

Abstract

The highly delocalized distribution of the MOs in C_{60} has been analyzed with the aid of extended Hückel calculations and their graphic representations. Symmetry and perturbation theory arguments rationalize the MO correlations in terms of the *implosion* of 12 C_5 rings distributed at the vertices of an expanded icosahedron. In particular, two distinguishable σ and π C_{60} subsets are each split into 30 filled and 30 empty MOs belonging to the same species under I_h symmetry. As a major difference, whereas 30 new C–C σ bonds add to the 60 pre-existing C_5 endocyclic bonds, some partial π bonding at the 6:6 edges of C_{60} occurs at the expense of π bonding at the 5:6 edges. This point has been clarified by referring to the electronic structure of the simpler molecule [5]-radialene which typifies the MO response to the idea of π resonance. An overview at the C–C bonding/antibonding roles in all of the π MOs simplifies understanding their possible interactions with the frontier MOs of typical transition metal fragments. The model complexes considered involve the η^2-coordination of the C_{2v} fragment $(PH_3)_2Pt$ to C_{60} in 6:1, 2:1 and 1:1 ratios. The MO analysis highlights the electronic causes of the deformation from sphericity of C_{60} when a metal is attached to one or more 6:6 edge. Attempts to explore alternative, but as yet unsynthesized coordination modes have also been made.

Key words: Fullerene; Metal complex; EHMO calculations; Qualitative MO theory

1. Introduction

The chemistry of fullerenes is rapidly growing [1] and the exploration of their electronic structure remains a fascinating task. The compactness of buckminsterfullerene with the rare I_h symmetry and the intrinsically high electron delocalization are a challenge to the description of the chemical bonding. Over the past few years, several quantum mechanical studies have appeared at all levels of sophistication [2]. Nevertheless, chemists require a simplified description which, in addition to the important concept of resonance focuses on the residual functionalities of single or grouped carbon atoms typical of elementary organic molecules. An important step towards an understanding of organometallic chemistry was made when the transition metal fragments began to be seen as functional groups which were isolobal with organic residues [3]. Growing experimental evidence that C_{60} can coordinate to some typical metal fragments [4] suggests that sufficiently localized MO frames exist on the surface of the pseudo-spherical molecule.

In this paper, we first present an overview of the major bonding components of the C_{60} skeleton. The computational method used is EHMO [5] but because of its well-known shortcomings, arguments based on the absolute energies, distribution of charges, etc. have generally been avoided. In contrast, we have tried to interpret as best we can the symmetry properties which are a major factor in determining the character of the various MOs. In particular, an increased understanding of the topological distribution of the carbon p_π orbitals helps to rationalize the regioselectivity of C_{60} in binding to metal fragments. Furthermore, the lost pseudo-sphericity of the C_{60} sphere upon coordination can be rationalized by some four-electron repulsions which compete with the binding forces. The CACAO package is an unique tool to display 3D representations of the MOs and their related properties on a computer screen [6].

Correspondence to: Dr. C. Mealli.

0022-328X/94/$7.00
SSDI 0022-328X(94)24503-B

2. Carbon–carbon bonding in C_{60}: σ and π frameworks

Buckminsterfullerene is a truncated icosahedron. Thus, a way of visualizing C_{60} and the ideal genesis of its MOs, is to imagine the *implosion* (see I) of an infinitely expanded icosahedron whose vertices are the comparably dimensionless C_5 rings (assumed C–C average distance = 1.40 Å).

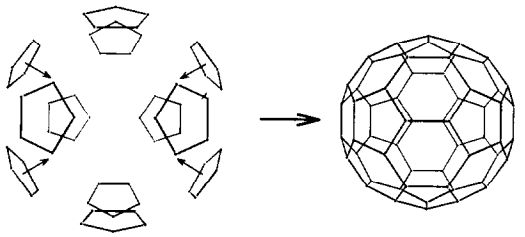

I

By maintaining the I_h symmetry, modelling of the process is finalized when the separation between any pair of carbon atoms from two different rings has become equal to the C–C intra-ring distance. Such a constraint for the final C_{60} model is consistent with idea that, at the extended Hückel level, it is better to avoid any structural bias. Indirectly, the calculated overlap populations indicate which type of C–C edges prefer to be shorter. The reliability of the computation is confirmed by the smaller overlap population of the C_5 endocyclic bonds with respect to the bonds (exocyclic) which connect two different five-membered rings (0.99 *vs.* 1.05). Most important, however, monitoring the levels along the ideal *implosion* pathway helps to classify the overall C–C bonding/antibonding features.

Each carbon atom of the C_5 ring is characterized by in-plane (σ, sp^2 hybrid, **II**) and upright ($\pi_\perp$, **III**) orbitals which eventually form two distinguishable tangential (σ) and radial (π) networks with a total of 60 MOs in each. Although such a distinction is not rigorous, since mixing between σ and π components occurs along the implosion pathway, the ideal relation with more elementary systems greatly simplifies the problem (*e.g.* olefins with separate σ and π components unquestionably set the C–C bond order at two).

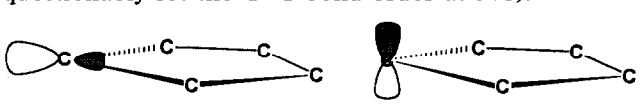

II **III**

In the isolated C_5 ring, the D_{5h} symmetry groups five σ hybrids of type **II** into a'_1, e'_1 and e'_2 classes, as shown in **IV**.

Although e'_2 contains two nodal planes orthogonal to the C_5 plane (δ-type function), it is almost degenerate with e'_1 which has only one node (p-type function). This is attributable to the small size of the orbital lobes overlapping inside the ring. Only a'_1, which is an overall in-phase combination of the five hybrids (s-type function), is stabilized with respect to the other FMOs by *ca.* 1.8 eV.

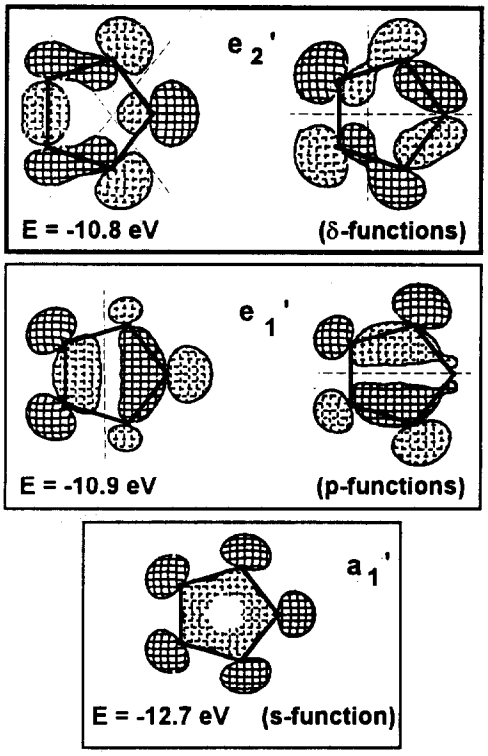

IV

The FMOs **IV** have little effect on the endocyclic C_5 σ bonding which is largely due to the reciprocal interactions between the two additional sp^2 hybrids at each carbon atom (not shown). Accordingly, the FMOs **IV** remain almost entirely available for exocyclic bonding. The bonding/antibonding interactions of the latter with symmetry-adapted combinations of H_{1s} orbitals in C_5H_5 (radical or anion) are almost a trivial example. It is not nearly so easily to visualize the same FMOs forming the exocyclic C–C bonds of C_{60}, although the situation is basically similar to that in cyclopentadienes.

Figure 1 shows a Walsh-type diagram for the implosion of 12 C_5 rings. The I_h symmetry combinations of 12 sets of FMOs **IV** separate into two groups of 30 bonding and 30 antibonding MOs which quickly diverge. If each hybrid **II** is formally assigned one electron, the 30 bonding MOs are fully populated and 30 new C–C σ bonds ensue.

Since the generators of the actual MOs are s-, p- or δ-type functions, it would be useful to follow the relative weights of the latter along the implosion pathway.

Whereas the species A_g, T_{1g} and T_{2g} are generated by an unique basis function (s, p or δ), all other species involve the mixing of two or three different sets (e.g. H_g). This also implies avoided crossings or divergencies between isosymmetric levels. Fortunately, the analysis of simpler I_h molecules (see below) has enabled us to recognize the bonding/antibonding possibilities of the pure basis functions before any mixing. The trends for any symmetry species are highlighted by the circles and squares in the upper box of Fig. 2. The mixings can either increase or reduce a given trend, but in general good bonding interactions accompany significant divergencies between filled and empty levels. As shown in Fig. 1, this holds for the σ network, in which the mixings favoured by the closeness of energy of the basis FMOs **IV** take place as soon as the mutual overlaps become sufficiently large. The sets G_g, G_u and H_u (p + δ) as well as T_{1u} (s + p) and T_{2u} (s + δ) diverge into bonding and antibonding combinations. The three H_g sets correlate with one antibonding (empty) and two bonding (filled) MOs. Finally, the symmetry itself imposes bonding (A_g) and antibonding (T_{1g} and T_{2g}) characters as the genuine s, p and δ functions.

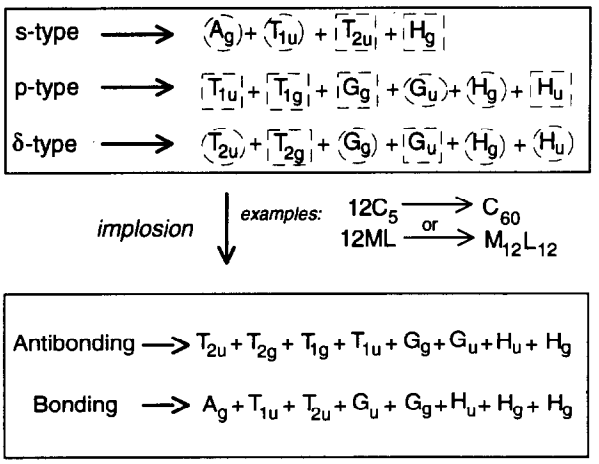

Fig. 2. In the upper box, a schematic representation of the I_h symmetry species obtainable from basis sets of atomic or fragment orbitals (e.g. C_5) with two (δ), one (p) and zero nodes (s), respectively. Circles or squares enclosing the labels indicate the bonding or antibonding character of the levels as determined from the relationship between the basis functions of a given type (before any mixing). In the lower box, the MOs of the final icosahedral molecule are grouped in terms of their overall bonding/antibonding character.

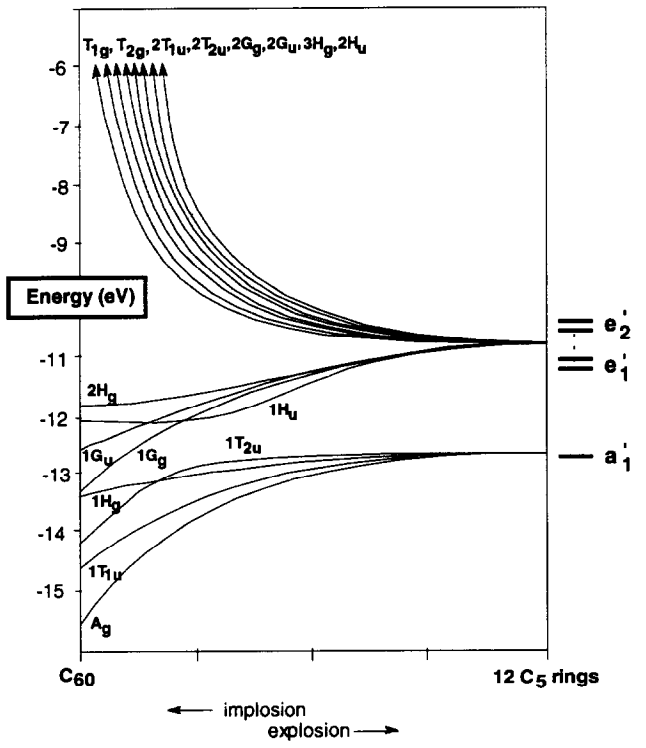

Fig. 1. The correlation between 12 sets of σ hybrids of the C_5 rings (see **IV**) during the formation of C_{60}.

As mentioned, the correlations between the C_{60} σ MOs can be distinguished by comparison with simple icosahedra of the type $M_{12}H_{12}$ (M = transition or non-transition element). The idea is that the carbon atoms of any C_5 ring can be imagined as collapsing into an unique central atom. Accordingly, the nodal properties of the basis functions in **IV** would coincide with the pure atomic orbitals d_{xy}, $d_{x^2-y^2}$, p_x, p_y, and s (with two, one and zero nodes, respectively).

If the M_{12} skeletal atoms have no accessible d orbitals, as is the case for the species $B_{12}H_{12}^{2-}$, the 30 B–B icosahedral edges cannot attain a bond order of 1 (shortage of orbitals or hypervalence). Indeed, the whole B_{12} bonding results from reciprocal interactions between 36 orbitals (one sp hybrid and p_x and p_y orbitals from any boron atom). As is well known [7], $B_{12}H_{12}^{2-}$ is characterized by 13 filled bonding ($A_g + H_g + T_{1u} + G_u$) and 23 empty antibonding ($H_g + T_{1u} + G_g + H_u + T_{2u} + T_{1g}$) MOs. In this case, only the H_g and T_{1u} combinations are generated by both the s and the p orbitals and a total of 8 + 8 bonding and antibonding levels arises from their reciprocal mixing. The filled bonding G_u set arises from the p orbitals alone. Similarly, the G_g and H_u symmetries from the p orbitals (as well as T_{1g}) are antibonding as for C_{60}. Finally, in the absence of mixing with δ-based levels, an intrinsic antibonding character is assigned to the s combinations of sp hybrids, T_{2u}. Needless to say, the same sp hybrids alone give rise to the overall bonding A_g MO.

The relationship between C_{60} and icosahedra formed by 12 transition metals is even more direct because of the availability of δ-basis functions. In principle, one electron could be formally assigned to any p_x, p_y, d_{xy} and $d_{x^2-y^2}$ orbital and to an sp_z hybrid to generate the 30 M–M bonds of a model such as $Au_{12}L_{12}$ (when L = a terminal two-electron ligand). Of the remaining four orbitals of each metal, one (outpointing sp_z hybrid) would receive electrons from the terminal ligand and the other three (d_{xz}, d_{yz} and d_{z^2}) would hold metal lone pair electrons. A major complication with such an ideal model, which should have 156 electrons, is the much lower energy of the δ orbitals with respect to the s and p. Thus, the appropriate pattern of 30 M–M bonding MOs (filled) below 30 antibonding ones (empty) cannot be attained and indeed the hypothetical model does not exist. However, 162e species such as $[Au_{12}Cl_2(PR_3)_{12}(\mu_{12}\text{-}Au)]^{3+}$, containing an interstitial atom, have been characterized [8]. A theoretical analysis of the latter (to be reported elsewhere [9]) describes the overall MO architecture using the methodology previously developed for octahedral metal clusters [10]. This gives information on role of the δ-type orbitals in the external Au_{12} framework. The information in the upper box of Fig. 2 could be completed by extrapolating some of these results to C_{60}.

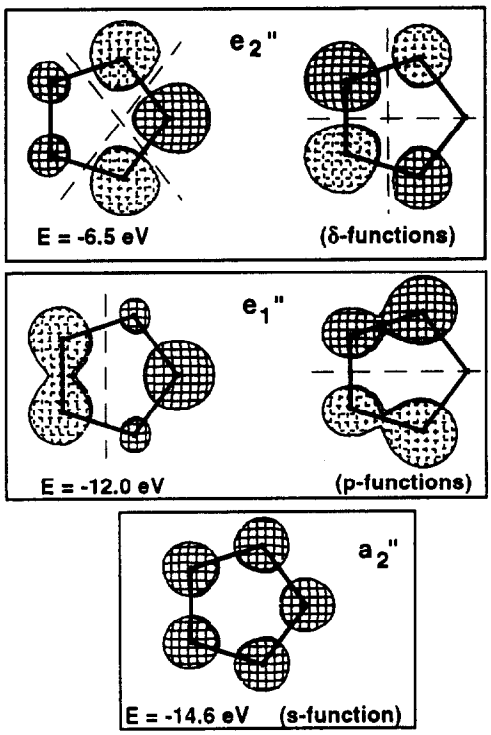

V

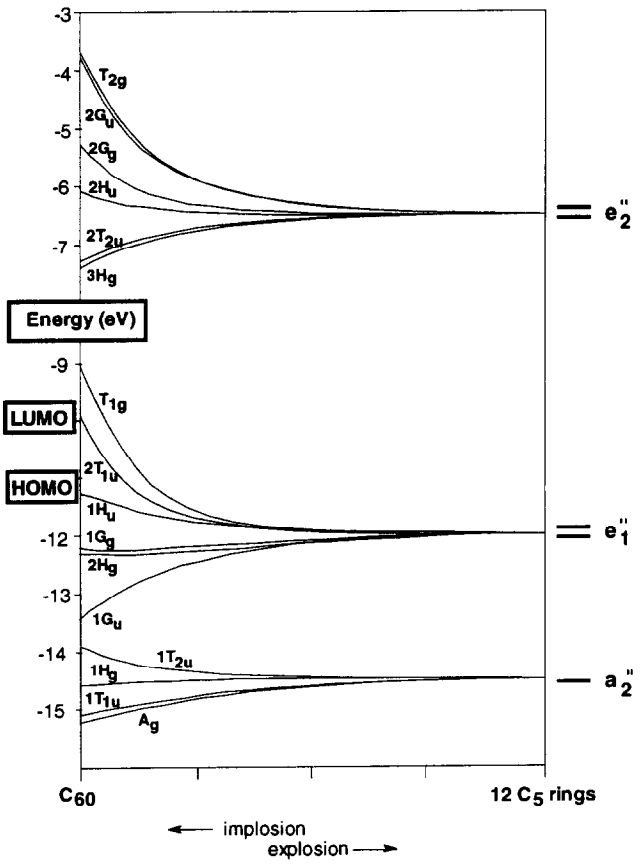

Fig. 3. The correlation between 12 sets of $\pi_\perp$ orbitals of C_5 rings (see V) during the formation of C_{60}.

The study of the intermixing between s-, p- and δ-type functions which underlies the C_{60} skeletal σ bonding is also a good basis for understanding the π framework formed by the carbon p_π orbitals, **III**. As shown in **V**, these organize in C_5 according to the symmetries a_2'', e_1'' and e_2'', the gaps a_2''–e_1'' and e_1''–e_2'' now being large (*ca.* 2.5 eV and 5.5 eV, respectively). It is worth recalling that the same C_5 π FMOs are involved in coordination of a cyclopentadienyl anion to a metal: The donation of the electrons from the FMOs a_2'' and e_1'' is most important but some back-donation into the higher e_2'' set also occurs. In this case (as well as in the formation of C_{60}), the antisymmetry of the $\pi_\perp$ orbitals with respect to the C_5 plane is not as crucial as the nodal properties with respect to the orthogonal planes which classify the FMOs a_2'', e_1'' and e_2'' as s-, p- and δ-type functions, respectively. For this reason all of the π MOs generated along the I_h pathway to buckminsterfullerene by the basis sets **V** have the same symmetries as the σ MOs **IV**.

The implicit trends of Fig. 2 do still apply, while the analogies and the differences between the σ and π frameworks can be highlighted by comparing the previous Walsh diagram of Fig. 1 with that of Fig. 3. In the

latter, the whole set 60 π MOs evolves (from right to the left) into 30 lower (filled) and 30 higher (empty) levels, the symmetry subsets being the same as in the lower box of Fig. 2. Also, the final separation between H_u and T_{1u} (the π-type HOMOs and LUMOs) compares with several previous calculations and is large enough (*ca.* 1.3 eV) to provide thermodynamic stability to C_{60}. Even so, the filled and empty π levels do not attain the distinct exocyclic bonding/antibonding characteristics observed in the σ subset. Certainly, the implosion does not lead to the formation of as many as 30 new C–C π bonds and in no case can the 5:6 (C_5 endocyclic) and 6:6 (exocyclic) edges be assigned the limiting bond orders of 1 and 2, respectively.

Whereas the formation of single exocyclic σ bonds is made possible by the dedicated sp^2 hybrids **I** (endocyclic bonding is assured by two additional sp^2 hybrids), the single π orbital per carbon atom (**II**) implies that any new exocyclic π bond (or portion of it) occurs at the expenses of an endocyclic one. This also occurs in the much simpler [5]-radialene, even though X-ray analysis [11] shows that in this molecule the endocyclic C_5 linkages are definitely longer than the external ones to methylenes (1.50 *vs.* 1.35 Å). In C_{60}, the difference between 5:6 and 6:6 edges is much less significant (1.45 *vs.* 1.39 Å, respectively [12]).

A diagram (**VI**) of the π interactions between the C_5 orbitals **V** and the symmetry-adapted combinations of five methylene groups, shows five strong bonding/antibonding interactions of a_2'', e_1'' and e_2'' type. In particular, the C_5 a_2'' FMOs (overall bonding for C_5) and e_1'' (predominantly, but not exclusively, endocyclical bonding) redirect a good part of their electron density towards the methylenes (see an example in **VII**). At the same time, the C_5 antibonding e_2'' FMOs become partially populated. The filled MOs account for most of the C=C double bonds to methylenes. However, the endocyclic C_5 π bonding is not zero, as shown by one of the $1e_1''$ MOs (**VII**) which, in part, maintains the endocyclic bonding character of the original e_1'' FMO shown in **V**. If this is true for [5]-radialene, even more C_5 double-bond character remains in C_{60}. In fact, given the single C–C distance of 1.40 Å, reduced overlap values of 0.87 and 1.24 may be calculated for the *endo* and *exo* bonds of [5]-radialene, whereas the corresponding C_{60} values are 0.98 and 1.05, respectively.

A diagram similar to **VI** in which FMOs **V** interact with those of the fragment C_{55} is not very useful for interpreting the C_{60} π bonding because the C_{55} FMOs are themselves complicated combinations of 11 sets of type **V**. Thus, the correlation diagram for the implosion

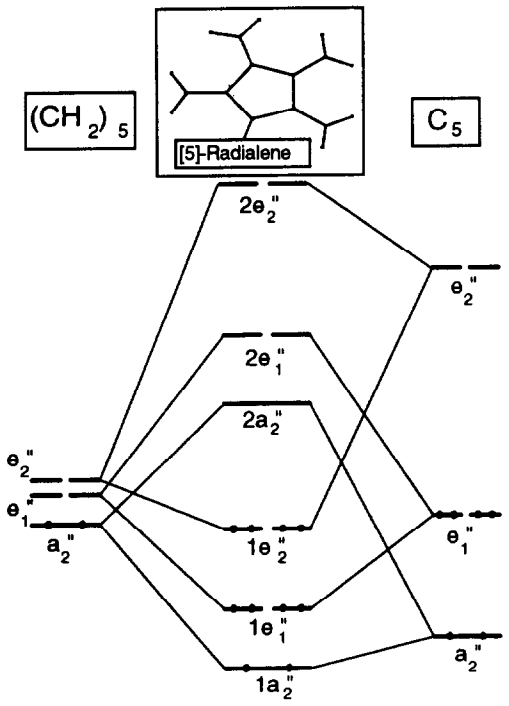

VI

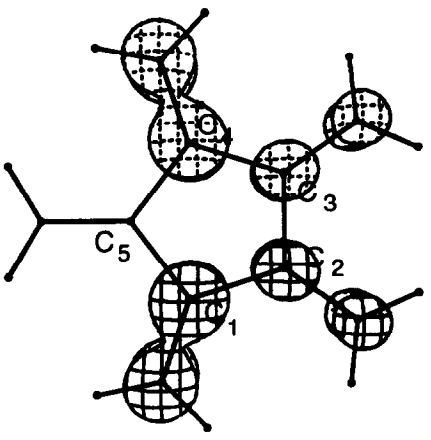

VII

Form 5.

in Fig. 3 is more significant. Because of the large energy gaps between the C_5 components **V** and the poor overlap between adjacent p_π atomic orbitals even when the exocyclic C–C separations become small, the intermixing between the s, p and δ basis functions is not as large as in the σ network (Fig. 1). Ultimately, all the π MOs share 5:6 and 6:6 edge bonding and antibonding character, the relative weights being difficult to determine. The following aspects are emphasized:

(i) The unique A_g MO, which is already endocyclically bonded, drops in energy on acquiring additional exocyclic bonding character.

(ii) The filled and empty T_{1u} sets diverge, $2T_{1u}$ becoming the LUMO of C_{60}. The exocyclic bonding and antibonding trends of the pure s and p T_{1u} functions (see upper part of Fig. 2) are increased by the reciprocal mixing. Consistent with the idea proposed for [5]-radialene, three endocylic bonds become partially exocyclic. Drawing **VIII** of a $2T_{1u}$ member shows a small central s-type contribution, which is antibonding with respect to the adjacent p-type functions (upper C_{60} hemisphere viewed down the five-fold axis). An equivalent linear combination of the same MO (shown later) highlights the π^* character localized at the two antipodal 6:6 edges even better. The latter representation is indeed more appropriate for describing positive bonding interaction with transition metal fragments.

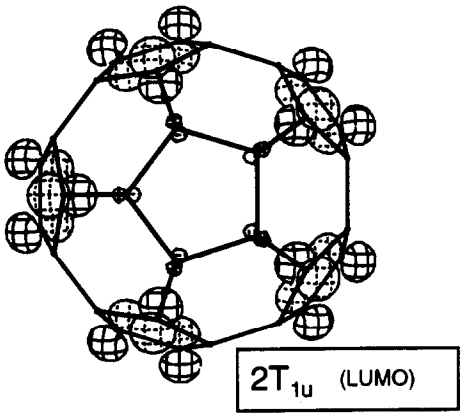

VIII

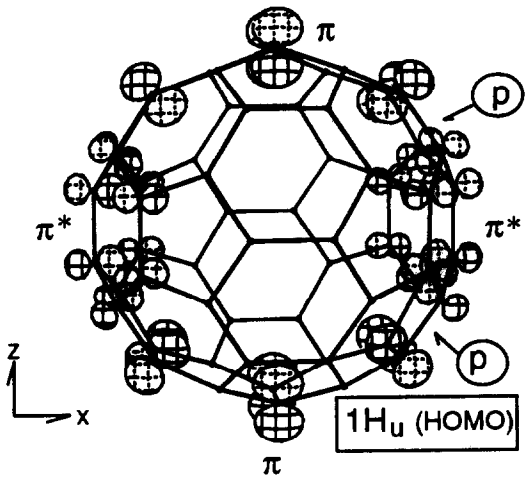

(iii) The G_u, G_g and H_u species split pairwise into filled and empty sets by mixing their p and δ characters. In particular, the $1G_u$ set (the original p-based set is weakly bonding) is definitely stabilizing. The behaviour of the filled $1G_g$ and $1H_u$ MOs is instead more flattened. Their basic p-type components are exocyclically antibonding and hence destabilizing; such a trend is modulated but not reversed by mixing of the bonding higher δ components [13*]. Drawing **IX** shows that the two characters π and π^* coexist in one member of the HOMO ($1H_u$) at the 6:6 edges perpendicular to the z and x axes, respectively. In particular, the localized π^* character stems from a combination of two original C_5 p-type functions (*cf.* the left-most e_1'' FMO in **V**). Unfortunately, the δ contribution which localizes π bonds at the other edges is not so evident in the drawing. It will be shown below that the π and π^* dicotomy in the HOMO has some important consequences for the attachment to C_{60} of metallic fragments or other groups. Regardless of the relative weights, the δ–p mixing in the various G_u, G_g and H_u MOs suggest 13 partial bonding interactions occurring at the exocyclic bonds.

(iv) The two T_{2u} levels appear to be converging rather than diverging. The respective antibonding and bonding trends of the original s and δ functions (see Fig. 2) also seem predominant because intermixing is made difficult by the large a_2''–e_2'' energy gap. The less the mixing, the more $1T_{2u}$ retains the original C_5 bonding character of the a_2'' FMO and the more interelectronic repulsions are triggered in exocyclic directions. Recall that in $B_{12}H_{12}$, for example, with no δ orbitals available the T_{2u} combination of s orbitals (antibonding) is high in energy. In C_{60}, $1T_{2u}$ is populated and, although some δ mixing probably avoids major destabilization, the level is mainly endocyclically bonding.

* Reference number with asterisk indicate a note in the list of reference.

(v) The assignment of definite roles for the three H_g levels is even more intriguing. In particular, the empty $3H_g$ parallels the behaviour of T_{2u}, and it stabilizes because the δ functions are bonding. Conversely, none of the two filled sets is clearly destabilizing despite the antibonding tendency of their basic components (see Fig. 2). Although it is difficult to assign relative weights, the 20 electrons in the H_g MOs contribute both to the 5:6 and 6:6 edge π bonding. Again, 10 exocyclic C–C π-bonding interactions, however weak, form at the expense of the endocyclic bonding.

(vi) The T_{1g} and T_{2g} levels stem only from pure p- and δ-type functions, respectively. Their increase in energy on implosion confirms the exocyclic antibonding trends which must be counterbalanced by bonding MOs (note that amongst the filled levels, A_g and at least one H_g set have no antibonding partner of the same symmetry). In particular, the π^* character of T_{1g}, similar to that of $2T_{1u}$ (second and first LUMOs, respectively), can localize at antipodal 6:6 edges (perpendicular to the horizontal axis for the T_{1g} member shown in **X**). Both T_{1g} and $2T_{1u}$ can make fundamental interactions with metal d_π orbitals.

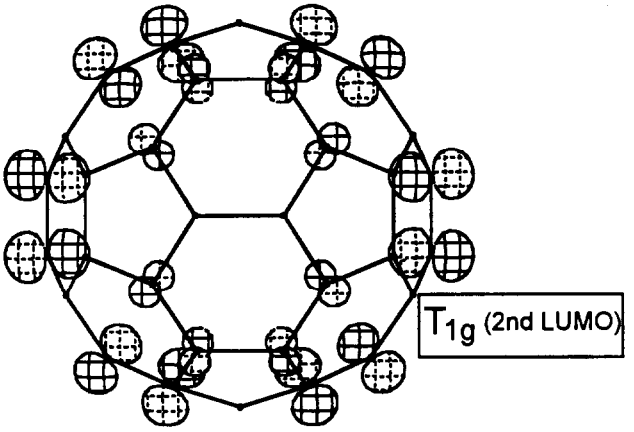

X

Summarizing, in C_{60} as well as in [5]-radialene the π MOs cannot be separated into two groups responsible for C_5 endocyclic and exocyclic bonding. In contrast, the C–C bond orders would be defined if the relative incidence of any populated MO in each type of bond was known Here we have only addressed the qualitative MO viewpoint which can be related to the concept of resonance invoked by some authors for C_{60} [14]. With reliable values of the C–C overlap populations, the EHMO method can show how the basis sets (the π FMOs of the C_5 rings) combine in terms of symmetry and perturbation theory. Some idea has been acquired about the role of the different highly delocalized C_{60} MOs. This is a necessary preliminary to any analysis of the interactions of C_{60} with transition metal fragments.

3. The bonding interactions of C_{60} with transition metal fragments

The rapid development of C_{60} organometallic chemistry [4] has indicated that single or pairs of antipodal 6:6 edges are the favoured sites for dihapto coordination, the most suitable metal fragments being of the types L_2M and L_4M with C_{2v} symmetry, *e.g.* $(PR_3)_2M$ (M = Ni, Pd or Pt; d^{10}) or $[X(CO)(PR_3)_2M]^+$ (M = Rh or Ir, d^8 X = C or H The frontier orbitals of these fragments are *isolobal* and consist of a high σ hybrid and a lower hybridized and filled d_π orbital [15]. The same fragments are well suited to interact with olefins *via* combined donation and back-donation.

Our model complexes are 1:1, 1:2 and 1:6 adducts of C_{60} with $(PH_3)_2Pt$. Although the most complicated (378 MOs), the hexametallic species with the highest T_h symmetry is first considered. Figure 4 shows the major interactions between the frontier MOs of C_{60} with those of six $(PH_3)_2Pt$ fragments. The metal d_π FMOs are grouped according to the $T_u + T_g$ symmetries and find suitable energy and symmetry matches with the LUMOs of C_{60}. Recall that the latter sets with original $2T_{1u}$ and T_{1g} symmetries have π^* character at pairs of antipodal 6:6 edges. In C_{60}, as well as in the olefin complexes, back-donation to the C–C π^* orbital is synergistic with donation from the corresponding π-bonding partner into a metal σ hybrid. Figure 4 shows that the latter type of interaction with T_u, A_g

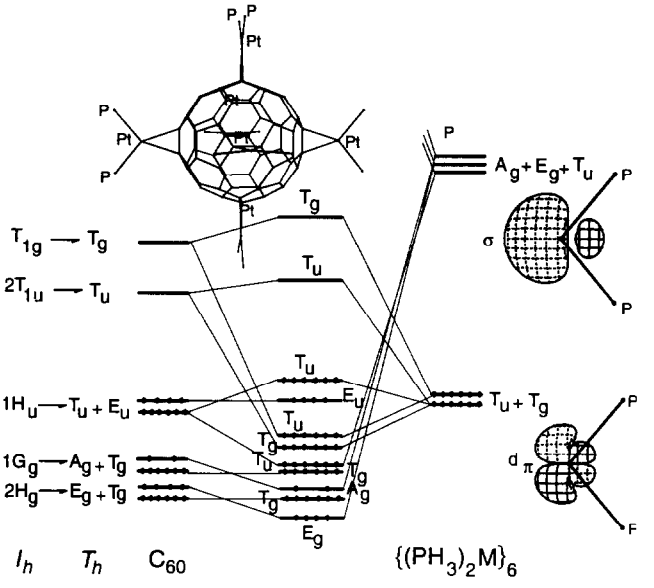

Fig. 4. The interaction between buckminsterfullerene and six $Pt(PH_3)_2$ fragments disposed according to T_h symmetry.

and E_g symmetries involves the C_{60} orbitals deriving from $1H_u$, $1G_g$ and $2H_g$ sets. From the previous analysis of the C_{60} π system, no filled MO has predominant π-bonding character at the 6:6 edges. To compensate for the poor localization, additional T_u, A_g and E_g MOs (from the $1G_u$, A_g and $1H_g$ sets) donate electron density to the high-lying σ hybrids of the metals. For the sake of simplicity, the latter interactions are not shown in Fig. 4.

The HOMO of the complex (T_u) is somewhat destabilized by the antibonding interaction between the filled metal d_π orbitals and the T_u set of C_{60} which arises from $1H_u$. Remarkably, both the latter FMOs are already involved in the donation back-donation interactions fundamental to the formation of the complex. This can be explained by recalling from **IX** that H_u members have dual σ and π features at 90° apart. What is good for σ bonding in one direction, induces a four-electron destabilization of a π type in the other. It can be shown that this is the major cause of perturbation for all of the C_{60} metal complexes as well as for fulleroids [16] in which a (such as osmyl [17], methylene, diazoalkane, *etc.* [16]) is attached to C_{60}. The effect is to lengthen the η^2 C–C bond by *ca.* 0.15 Å in metal adducts, by 0.20–0.25 Å in Diels–Alder adducts [18] and by as much as *ca.* 0.5 Å in $(4\text{-}BrC_6H_4)_2C_{61}$ [16]. Also the C–C edge is pulled out of the pseudospherical surface [4].

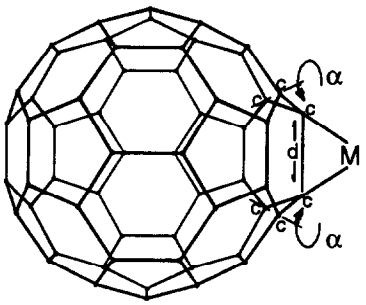

XI

In metal–olefin complexes, progressive lengthening of the C=C double bond with increasing π-back-donation is well understood, as is the repulsion from the metal of the two CH_2 planes in a metallacyclopropane adduct. In the C_{60} complexes, the two C_3 groups formed by one atom linked to the metal and to two neighbours which are not coplanar, cannot be pushed further back (*i.e.* rotated about the axis passing through the coordinated carbon atom and perpendicular to the MC_2 ring). However, each C_3 plane has an alternative degree of freedom, a rotation hinged at the axis defined by the two uncoordinated C atoms as schematically represented in **XI**. In this way, it is possible to obtain the experimentally observed structural deformation.

For the sake of simplicity, we examine the effects of perturbation alone for the mononuclear complex

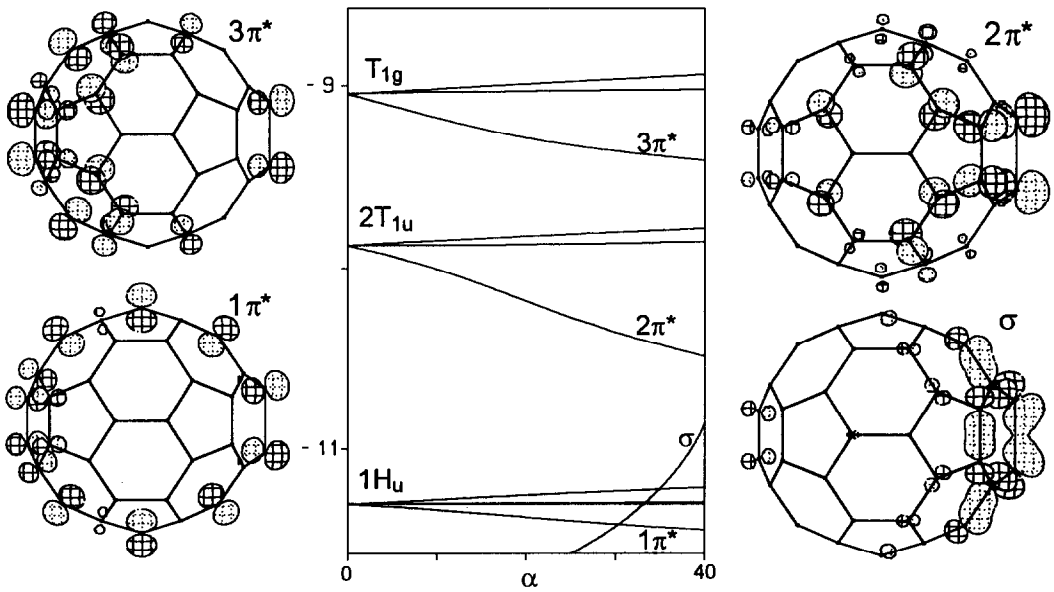

Fig. 5. The evolution of the C_{60} frontier MOs on elongating one 6:6 edge through the simultaneous rotation of two C-3 planes connected by the edge itself (see drawing **XI** in the text). The orbital diagrams clarify the behaviour of the most affected levels.

$(PH_3)_2Pt(\eta^2\text{-}C_{60})$ in which the lengthening of the coordinated C–C bond is more pronounced than in the hexanuclear analogue (1.54 *vs.* 1.49 Å) [4c]. The bonding interactions between the metal fragment and the undeformed C_{60}, although complicated by some mixing due to the lower C_{2v} symmetry, follow the indications of Fig. 4. Thus electron donation into the high metal σ hybrid involves several filled MOs with π character at the specified 6:6 junction. The π back-donation involves two single members from $2T_{1u}$ and T_{1g} which intermix and become destabilized. The HOMO is now a single level, destabilized from the antibonding interaction between one $1H_u$ member and the metal d_π orbital (four-electron repulsion).

When α deformations are applied to the metal complex (with the Pt–C distances remaining unchanged), a well-defined minimum of *ca.* 0.7 eV is found for α *ca.* 15°. For larger angles the energy rises steeply. The optimized C–C distance is somewhat longer than the experimental (*ca.* 1.65 Å) but the trend is reassuringly correct. Incidentally, a calculation for the fulleroid $(4\text{-}BrC_6H_4)_2C_{61}$ (a result not further discussed here) shows a minimum very close to the value of *ca.* 1.84 Å for the C–C distance reported in the experimental structure [16].

The MO basis of the energy minimum are contained in the Walsh diagram (Fig. 5) for the opening of one 6:6 edge in the free C_{60} molecule *via* the two α rotations. Three MOs, shown in the figure, arise from the T_{1g}, $2T_{1u}$ and $1H_u$ sets. All stabilize because of the reduced π^* character. In particular, upon decreasing the energy gap the empty $3\pi^*$ and $2\pi^*$ levels become better suited for interaction with the metal d_π FMO. For the converse reason, the filled $1\pi^*$ level becomes less repulsive towards that metal FMO and also because their overlap is reduced by the diverging orientations of the p_π orbitals in $1\pi^*$ (see Fig. 5). In the complex, the antibonding H_u/d_π level stabilizes and eventually loses its original HOMO identity. Upon deformation, and because of the reorientation of the sp^2 hybrids (**I**), the new HOMO can become a C–C σ level with rapidly increasing energy (see Fig. 5). Evidently, whenever a group is attached to C_{60}, the energy minimum stems from a balance between the optimum π-type interactions and the destabilization within the C_{60} σ network. The correct energetics may not be properly evaluated in all cases by the EHMO method, but the origin of the affect seems reliably identified.

As seen in Fig. 5, single members of T_{1g} and $2T_{1u}$ sets are stabilized when the deformation **XI** is applied to C_{60}. The energy gained by these levels is even larger if both the antipodal edges are opened up. These effects on edge stretching also apply to other members of the T_{1g} and $2T_{1u}$ sets, so it seems reasonable that deformations of this sort are triggered if there are electrons in the levels. This may be the case for the reduced derivatives of C_{60} (with up to six electrons) [19] and for the alkali-doped fullerides [2o]. In a similar manner to the monometallic complex, a well-defined total energy minimum is calculated for α rotations of *ca.* 10° in the C_{60} monoanion. If this is the case, anionic fullerenes should be characterized by little cuts or holes in the pseudo-spherical surface.

Finally, the regioselectivity of coordination of a second metal fragment at C_{60} has been debated in the literature [4]. Recent structural evidence [4d] shows that the preferential disposition of two metal fragments is at two antipodal 6:6 junctions. Our EHMO calculations also indicate that such a conformer is slightly preferred with respect to one in which the two metal fragments are coordinated at 90° apart. A qualitative explanation is again provided by the stabilizing trends of the π^* levels of C_{60} upon the deformation **XI**. Drawing **XII** shows the π^* metal–C_{60} antibonding level of the complex $(PH_3)_2Pt(\eta^2\text{-}C_{60})$ which should, in principle, be the third LUMO (destabilized over the other two unperturbed $2T_{1u}$ FMOs of C_{60}). Consistent with other calculations on $(PH_3)_2Pt(\eta^2\text{-}C_{60})$ [20], the original π^* character of the 6:6 edge furthest from the metal is barely perturbed so that stabilization of the level could occur upon deformation of type **XI** at that edge. Eventually this can become the actual LUMO, then available for d_π interaction with a second metal.

The other two unperturbed LUMOs are also susceptible to similar stabilizations and in principle any one of the four 6:6 edges 90° away from the first metal could be coordinated. Nevertheless, opening of the *trans*-metallic 6:6 edge is implicit in the coordination of the first metal. In fact, the $2T_{1u}$ FMO of C_{60} involved in **XII** already receive back-donation from the first metal coordinated. The metal–C_{60} bonding partner of **XII** is populated and gains energy if the π^*

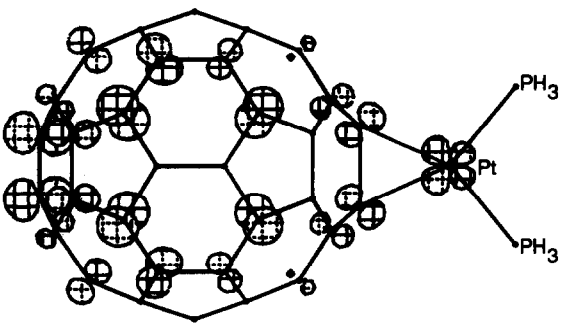

XII

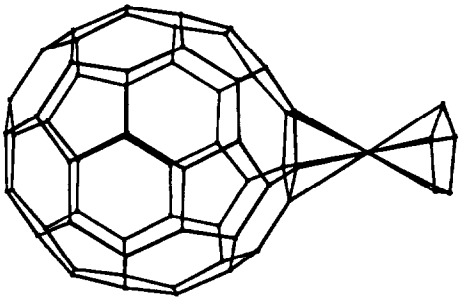

XIII

character of the antipodal 6:6 edge can be relieved by such geometric perturbation.

4. Conclusions and extentions

The highly delocalized distribution of MOs in C_{60} has been analyzed by pictorial representations obtainable from EHMO calculations. Symmetry and perturbation theory arguments have been largely used in an attempt to reveal residual functionalities at the surface of C_{60} which in turn promote the coordination of transition metal fragments. It has been pointed out that some MOs develop π-bonding/antibonding character at the 6:6 edges but there is also an echo of the original C_5 ring π system in many MOs. In this respect, the $2T_{1u}$ (LUMO) and $1H_u$ (HOMO) frontier levels have been shown to have the nodal properties of the isolated C_5 rings (for example, the p-type functions appear in **VIII** and **IX**) at some places. The second T_{1g} LUMO in C_{60} (**X**) is also a combination of pure C_5 p-type functions. Accordingly, we have considered the alternative coordination of a metal above the centre of one C_5 ring. Fragments of CpM type or the isolobal L_3M with two degenerate d_π orbitals [15] may be suitable.

A preliminary calculation of the hypothetical adduct $[CpNi(\eta^5\text{-}C_{60})]^-$ (see **XIII**) indicates the expected significant positive interactions between the filled d_π orbitals of nickel (d^{10}) and members from the LUMOs of C_{60}. However, there are strong four-electron repulsions between the same two metal d_π orbitals and members of the $1H_u$ HOMO which also carry p-type functionality at certain C_5 rings (see **IX**). Because of the latter, the doubly degenerate HOMO is pushed to too high an energy for the complex to be stable. In contrast, the $1H_u$–d_π four-electron repulsions change to attractive interactions in a complex such as $[CpFe(\eta^5\text{-}C_{60})]^+$ with four electrons less (the metal is d^6 and the two d_π orbitals are empty). The previously degenerate HOMO is now the LUMO, which is separated in turn from the new HOMO by slightly more than 1 eV. The calculated energy gain for the $CpFe^+$–C_{60} interaction is *ca.* 2 eV.

However, it can also be argued that π-acceptor rather than π-donor metals leave too much carbocationic character at C_{60} since the original LUMOs remain uninvolved and empty. Moreover, the pseudosphericity of the molecule may be perturbed unpredictably, with unknown effects on the energetics of the complex. Even though the previous arguments may not be quantitatively reliable for predicting new stable complexes, they represent a strategy for the future exploration of the coordination chemistry at C_{60}. Alternative regioselectivities or hapticities (η^3, η^4, η^6) are suggested by the topology of selected MOs (a detailed examination of the pictorial representations is not reported here) and could all be tested. Even if they are only metastable, certain adducts could at least be involved in haptotropic rearrangements of a metal and the spherical molecule.

Acknowledgements

Part of this work has been supported by the Progetto Finalizato Chimica Fine II (C.N.R.). The work of J.A.L. (c/o ISSECC) has been made possible by a scholarship provided by the Ministerio de Educación y Ciencia of the Spanish Government.

References and notes

1 For recent overviews, see (a) H.W. Kroto, *Angew. Chem., Int. Ed. Engl., 31* (1992) 111; (b) A. Hirsch, *Angew. Chem., Int. Ed. Engl., 32* (1993) 1138.

2 (a) A.D.J. Haymet, *Chem. Phys. Lett., 122* (1985) 421; (b) R.C. Haddon, L.E. Brus and K. Raghavachari, *Chem. Phys. Lett., 125* (1986) 459; (c) R.L. Dish and J.M. Schulman, *Chem. Phys. Lett., 125* (1986) 465; (d) S. Satpathy, *Chem. Phys. Lett., 130* (1986) 545; (e) D.S. Marynick and S. Estreicher, *Chem. Phys. Lett., 132* (1986) 383; (f) P.W. Fowler and J. Woolrich, *Chem. Phys. Lett., 127* (1986) 78; (g) M.D. Newton and R.E. Stanton J. Am. Chem. Soc. 108 (1986) 2469. (h) P.D. Hale, *J. Am. Chem. Soc., 108* (1986) 6087; (i) I. Laszlo and L. Udvardi, *Chem. Phys. Lett., 136* (1987) 418; (j) H.P. Lüthi and J. Almlöf, *Chem. Phys. Lett., 135* (1987) 357; (j) P.W. Fowler, P. Lazzaretti and R. Zanasi, *Chem. Phys. Lett., 165* (1990) 79; (k) R.C. Haddon and V. Elser, *Chem. Phys. Lett., 169* (1990) 362; (l) G.E. Scuseria, *Chem. Phys. Lett., 176* (1991) 423; (m) R. Sachidanan and A.B. Harris, *Phys. Rev. Lett., 67* (1991) 1447; (n) M. Haeser, J. Almlöf and G.E. Scuseria, *Chem. Phys. Lett., 181* (1991) 497; (o) R.C. Haddon, *Acc. Chem. Res., 25* (1992) 127.

3 R. Hoffmann, *Angew. Chem., Int. Ed. Engl., 21* (1982) 711.

4 (a) P.J. Fagan, J.C. Calabrese and B. Malone, *Science, 252* (1991) 1160; (b) *ibid., J. Am. Chem. Soc., 113* (1991) 9408; (c) *ibid., Acc. Chem. Res., 25* (1992) 134; (d) A.L. Balch, J.W. Lee, B.C. Noll and M.M. Olmstead, *J. Am. Chem. Soc., 114* (1992) 10984; (e) *ibid., Angew, Chem., Int. Ed., 31* (1992) 1356; (f) V.V. Bashilov, P.V. Petrovskii, V.I. Sokolov, S.V. Lindeman, I.A. Guzey and

Y.T. Struchkov, *Organometallics, 12* (1993) 991; (g) A.L. Balch, J.W. Lee, B.C. Noll and M.M. Olmstead, *Inorg. Chem., 32* (1993) 3577.
5 (a) R. Hoffmann, *J. Chem. Phys., 39* (1963) 1397; (b) R. Hoffmann and W.N. Lipscomb, *J. Chem. Phys., 36* (1962) 2179; (c) *ibid., J. Chem. Phys., 36* (1962) 2872.
6 C. Mealli and D.M. Proserpio, *J. Chem. Educ., 67* (1990) 399.
7 D.M.P. Mingos and D.J. Wales, *Introduction to Cluster Chemistry*, Prentice-Hall, Englewood Cliffs, 1990, p. 183, and references therein.
8 C.E. Briant, B.R.C. Theobald, J.W. White, L.K. Bell and D.M.P. Mingos, *J. Chem. Soc., Chem. Commun.*, (1975) 859.
9 J.A. Lopez and C. Mealli, unpublished results.
10 J.A. Lopez, C. Mealli, Y. Sun and M.J. Calhorda, *Inorg. Chim. Acta, 213* (1993) 199.
11 M. Iyoda, H. Otani, M. Oda, Y. Kai, Y. Baba and N. Kasai, *J. Chem. Soc., Chem. Commun.*, (1986) 1794.
12 (a) H.-B. Bürgi, E. Blanc, D. Schwarzenbach, S. Liu, Y. Lu, M.M. Kappes and J.A. Ibers, *Angew. Chem., Int. Ed. Engl., 31* (1992) 640; (b) M.F. Meidine, P.B. Hitchcock, H.W. Kroto, R. Taylor and R.M. Walton, *J. Chem. Soc., Chem. Commun.*, (1992) 1534.
13 A complication for the $1H_u$ HOMO arises from the energetically close H_u set of the σ type. The ill-behavior of latter in Fig. 1 is due to the unavoidable $\sigma-\pi$ intersystem crossing and confirms that a rigorous separation of the two frameworks is only an ideal.
14 D.J. Klein, T.G. Schmalz, G.E. Hite and W.A. Seitz, *J. Am. Chem. Soc., 108* (1986) 1301.
15 T.A. Albright, J.K. Burdett and M.-H. Whangbo, *Orbital Interactions in Chemistry*, Wiley, New York, 1985.
16 (a) F. Wudl, *Acc. Chem. Res., 25* (1992) 157; (b) T. Suzuki, Q. Li, K.C. Khemani and F. Wudl, *J. Am. Chem. Soc., 114* (1992) 7301; (c) S. Shi, K.C. Khemani, Q. Li and F. Wudl, *J. Am. Chem. Soc., 114* (1992) 10656.
17 J.M. Hawkins, *Acc. Chem. Res., 25* (1992) 150.
18 Y. Rubin, S. Khan, D.I. Freedberg and C. Yeretzian, *J. Am. Chem. Soc., 115* (1993) 344.
19 (a) P.-L. Allemand, A. Koch, F. Wudl, Y. Rubin, F. Diederich, M.M. Alvarez, S.J. Anz and R.L. Whetten, *J. Am. Chem. Soc., 113* (1991) 1050; (b) Q. Xie, E. Pérez-Cordero and L. Echegoyen, *J. Am. Chem. Soc., 114* (1992) 3978.
20 D.L. Lichtenberger, L.L. Wright, N.E. Gruhn and M.E. Rempe, *Synth. Met.*, (1993), in press.
21 J.H. Ammeter, H.B. Bürgi, J.C. Thibeault and R. Hoffmann, *J. Am. Chem. Soc., 100* (1978) 3686.
22 S. Alvarez, *Table of Parameters for Extended Hückel Calculations*, Departamento de Quimica Inorganica, Universidad de Barcelona, 1989.
23 N. Koga and K. Morokuma, *Chem. Phys. Lett., 202* (1993) 330.
24 H. Fujimoto, Y. Nakao, K. Fukui *J. Mol. Struct. 300* (1993) 425.

Appendix

Calculations of the extended Hückel type were carried out using a modified version of the Wolfsberg–Helmholz formula [21]. The atomic parameters used were those of Alvarez [22]. An single C–C distance of 1.40 Å was used in all the calculations, unless stated otherwise. In the model complexes, the Pt–C and Pt–P bonds were fixed at 2.10 and 2.25 Å, respectively. While this paper was in press two new articles were published dealing with the theory of the transition metal complexes of C_{60} [23,24].